The May-Hegglin anomaly gene *MYH9* is a negative regulator of platelet biogenesis modulated by the Rho-ROCK pathway

Zhao Chen,[1,2] Olaia Naveiras,[3,4] Alessandra Balduini,[5] Akiko Mammoto,[6,7] Mary Anne Conti,[8] Robert S. Adelstein,[8] Donald Ingber,[6,7] George Q. Daley,[3,4] and Ramesh A. Shivdasani[1,2]

[1]Department of Medical Oncology, Dana-Farber Cancer Institute, Boston, MA; [2]Department of Medicine, Harvard Medical School, Boston, MA; [3]Division of Hematology and Oncology, Children's Hospital, Boston, MA; [4]Department of Biological Chemistry and Molecular Pharmacology, Harvard Medical School, Boston, MA; [5]Department of Biochemistry, University of Pavia, Fondazione Istituto di Ricovero e Cura a Carattere Scientifico Policlinico San Matteo, Pavia, Italy; [6]Vascular Biology Program, Children's Hospital, Boston, MA; [7]Departments of Pathology and Surgery, Harvard Medical School, Boston, MA; and [8]Laboratory of Molecular Cardiology, National Heart, Lung and Blood Institute, Bethesda, MD

The gene implicated in the May-Hegglin anomaly and related macrothrombocytopenias, *MYH9,* encodes myosin-IIA, a protein that enables morphogenesis in diverse cell types. Defective myosin-IIA complexes are presumed to perturb megakaryocyte (MK) differentiation or generation of proplatelets. We observed that *Myh9*$^{-/-}$ mouse embryonic stem (ES) cells differentiate into MKs that are fully capable of proplatelet formation (PPF). In contrast, elevation of myosin-IIA activity, by exogenous expression or by mimicking constitutive phosphorylation of its regulatory myosin light chain (MLC), significantly attenuates PPF. This effect occurs only in the presence of myosin-IIA and implies that myosin-IIA influences thrombopoiesis negatively. MLC phosphorylation in MKs is regulated by Rho-associated kinase (ROCK), and consistent with our model, ROCK inhibition enhances PPF. Conversely, expression of AV14, a constitutive form of the ROCK activator Rho, blocks PPF, and this effect is rescued by simultaneous expression of a dominant inhibitory MLC form. Hematopoietic transplantation studies in mice confirm that interference with the putative Rho–ROCK–myosin-IIA pathway selectively decreases the number of circulating platelets. Our studies unveil a key regulatory pathway for platelet biogenesis and hint at Sdf-1/CXCL12 as one possible extracellular mediator. The unexpected mechanism for *Myh9*-associated thrombocytopenia may lead to new molecular approaches to manipulate thrombopoiesis. (Blood. 2007;110: 171-179)

© 2007 by The American Society of Hematology

Introduction

MYH9 encodes myosin-IIA, a nonmuscle myosin heavy chain that assembles within actomyosin complexes and facilitates shape changes in diverse cell types.[1-3] Patients with autosomal dominant inherited *MYH9*-related disorders,[4-6] including the May-Hegglin anomaly,[7,8] exhibit macrothrombocytopenia and variable degrees of hearing loss, nephritis, and cataracts. These individuals experience mild bleeding symptoms as a result of reduced numbers of misshapen blood platelets that can be 2 to 5 times larger than normal.[9,10] In the May-Hegglin anomaly, macrothrombocytopenia is due to a defect in platelet release by megakaryocytes (MKs) in the bone marrow, but platelets that do form seem to circulate and function normally.[9-11] The *MYH9*-associated syndromes are thus regarded as disorders of thrombopoiesis,[12] and defective myosin-IIA complexes are presumed to perturb some aspect of MK differentiation, likely late in the course of cell maturation.

Polyploid MKs accumulate an enormous and complex cytoplasm before they assemble and release blood platelets. Two key processes are thought to govern the timing and execution of platelet release. Mature MKs travel within the bone marrow and come to lie close to sinusoidal vessels[13]; this process responds to cellular and humoral interactions, mediated in part by the chemokine stromal cell–derived factor 1 (Sdf-1 or CXCL12).[14-16] In their final stages, MKs extend long cytoplasmic projections called proplatelets and actively assemble nascent platelets at the tips of these structures.[17-19] Proplatelet formation (PPF) is preceded and accompanied by characteristic changes in cell shape, reorganization of the actin and microtubule cytoskeletons, and generation of intracellular force.[20]

As an abundant motor protein within MKs and the only representative of its family,[21] myosin-IIA is a good candidate mediator of proplatelet extension or platelet release. Biochemical studies suggest that certain N-terminal mutations found in patients with *MYH9*-related disorders reduce intrinsic ATPase activity,[22] whereas other common C-terminal mutations may compromise myosin filament formation.[23] Although both classes of mutations may interfere with myosin-IIA function, it is unclear whether monoallelic *MYH9* mutations produce clinical phenotypes as a result of haploinsufficiency or dominant-negative effects. The role of myosin-IIA in platelet assembly and release is hence uncertain.

Conventional myosin-II complexes contain a dimer of heavy chains, each associated with the myosin regulatory light chain (MLC). Phosphorylated MLC enhances actin-dependent myosin motor activity,[24] and 3 kinases can phosphorylate MLC: Rho-associated kinase (ROCK), myosin light chain kinase (MLCK), and p21-activated kinase.[24] Both ROCK and MLCK participate in platelet activation,[25-27] but their roles in MK maturation or platelet

© 2007 by The American Society of Hematology

biogenesis are unknown. Other advances point to the important contribution of the small-GTPase Rho in elongation and retraction of neurites in response to Sdf-1,[28,29] and morphologic similarities between neurite extension and PPF raise the possibility that Rho and ROCK also regulate PPF. Our investigation of mechanisms in *MYH9*-related disorders led to consideration of the role of ROCK in myosin-IIA regulation and suggested this possibility independently. Here, we describe studies that implicate a Rho–ROCK–MLC–myosin-IIA pathway as a negative regulator of platelet biogenesis and suggest a surprising explanation for compromised thrombopoiesis in the face of *Myh9* gene mutations.

Materials and methods

Reagents and plasmids

Enzyme inhibitors Y-27632, ML-7, and blebbistatin were purchased from Sigma-Aldrich (St Louis, MO), Sdf-1 from Peprotech (Rocky Hill, NJ), MLC antibody from Sigma-Aldrich, and myosin-IIA antibodies from BTI (Stoughton, MA) and Covance (Princeton, NJ). Human *MYH9* full-length, R1933X, and rod-domain cDNAs were cloned into *Bgl*II and *Eco*RI sites of the pMIB vector, which was constructed by replacing the internal ribosome entry site (IRES)-green fluorescent protein (GFP) fragment in pMIG (gift from D.G. Tenen, Harvard Institute of Medicine, Boston, MA) with IRES-Blasticidin using *Eco*RI and *Cla*I sites. GFP-fused forms were prepared by cloning cDNAs into pEGFP-C1 (Clontech, Palo Alto, CA), followed by subcloning into *Age*I and *Eco*RI sites of a modified pMSCV vector (Clontech), replacing the PGK promoter and puromycin-resistance cassette. GFP-fused chicken $D_{18}D_{19}$-MLC and human $A_{18}A_{19}$-MLC and $D_{18}D_{19}$-MLC were excised from pEGFP-N1 host vectors (Clontech) and subcloned into *Bgl*II and *Cla*I sites of pMIG, replacing the IRES-GFP cassette. Red fluorescent protein (RFP)–fused MLC mutants were cloned into dsRed2-N1 (Clontech), and then ligated into *Bgl*II and *Cla*I sites of pMIG depleted of the IRES-GFP cassette. RhoAv14 was cloned by polymerase chain reaction (PCR) amplification and introduced into *Bgl*II and *Eco*RI sites of pMIG.

Tissue and ES cell culture

MKs were cultured and purified as described previously.[30] Human umbilical vein endothelial cells (HUVEC) were cultured in EBM-2 medium (Cambrex, Baltimore, MD) at 37°C in 5% CO_2 atmosphere. $MYH9^{-/-}$ ES cells were generated by re-electroporation of $MYH9^{+/-}$ embryonic stem (ES) cells with the targeting construct[31] and selection of colonies at increased G418 concentration (2.5 mg/mL). MKs were differentiated from mouse ES cells with minor modification of published methods.[32,33] Briefly, 2×10^4 ES cells were cultured in α-Minimal Essential Medium (MEM) (Invitrogen, Carlsbad, CA) over a monolayer of OP9 stromal cells (gift from S. Shattil, University of California, San Diego, CA) that was plated 2 days earlier in α-MEM medium supplemented with 20% fetal bovine serum (FBS) (Gemini, Alachua, FL). Differentiation took place for 5 days before ES cell derivatives were transferred onto a fresh OP9 monolayer in α-MEM medium supplemented with 15% FBS (Stem Cell Technologies, Vancouver, BC, Canada) and 1% thrombopoietin (TPO)–conditioned medium.[34] Differentiation was continued for 3 additional days before cells, including MKs, were transferred to a layer of γ-irradiated (3000 cGy) S17 stromal cells (gift from K. Akashi, Dana-Farber Cancer Institute, Boston, MA). PPF was scored on days 9 through 11, counting the initiation of ES cell differentiation as day 0. PPF was scored using the following criteria (see Figure S6, available on the *Blood* website; see the Supplemental Materials link at the top of the online article): (1) MKs lacking filaments, even those with shape change or short buds, were regarded as PPF-negative; (2) typical PPF MKs are characterized by extension of multiple proplatelets, with the most filaments exceeding 10 μm in length; (3) abnormal PPF MKs were judged by the presence of small or dense clusters surrounding the cell body; however, MKs with 3 or more extended proplatelets were counted as typical PPF even if clustered filaments were also evident.

Hematopoietic transplantation and flow cytometry

C57BL6/J bone marrow was treated with RBC lysis buffer (Sigma-Aldrich), followed by negative selection with magnetic beads (Miltenyi, Auburn, CA) and phycoerythrin (PE)–conjugated lineage-specific antibodies (Gr1, B220, CD4, CD8, NK1.1, Ter119) to enrich for progenitors. Isolated cells were transduced with retrovirus once every 24 hours for 3 days in StemSpam media (Stem Cell Technologies) in the presence of stem cell factor, TPO, interleukin-11 (IL-11), and IL-6 (Peprotech). For fetal liver transplantation, livers were isolated from embryonic day 13.5 (E13.5) mouse embryos and transduced with retrovirus as with Lin⁻ bone marrow progenitors. Six- to 10-week-old C57BL/6J female mice were given 2 doses of 550-cGy γ-irradiation separated by 3 hours, followed by retro-orbital sinus coinjection of retrovirus-transduced hematopoietic progenitors and 1.5×10^5 helper bone marrow mononuclear cells from age-matched C57BL6/J females. Mice were kept in a sterile environment for 6 weeks, with retro-orbital sinus blood sampling between 3 and 6 weeks, followed by euthanasia to analyze spleen and bone marrow. Total engraftment was evaluated as GFP⁺ cells within the CD45⁺ fraction, and multilineage engraftment as GFP⁺ cells in the myeloid Gr1⁺Mac1⁺ and lymphoid CD3⁺CD19⁺ compartments. Donor-derived MKs and platelets were identified on the basis of GFP⁺CD61⁺ signals in blood, spleen, or marrow samples that were disaggregated, diluted, and stained in acid citrate dextrose buffer, as described elsewhere.[35] All antibodies were purchased from BD Biosciences (San Diego, CA) and flow cytometry was performed in a BD Biosciences FACSCalibur instrument. Studies were approved by institutional animal care committees.

Retroviral infection

Retroviruses were produced by cotransfecting viral and PCL helper plasmids[36] into 50% to 70% confluent 293T cells using Fugene-6 (Roche, Palo Alto, CA). Medium was changed 24 hours later, and viral supernatants were harvested at 48 and 72 hours. Fetal liver cells were cultured with TPO-conditioned medium overnight before exposure to viral supernatants in the presence of 8μg/mL polybrene (Sigma-Aldrich) by centrifugation at 800*g* at 25°C for 90 minutes and incubation at 37°C for 1.5 hours. Cells were cultured in fresh TPO-conditioned medium for 2 days before isolation of advanced MKs over a bovine serum albumin (BSA) step-gradient[30] for further analysis. ES cell–derived hematopoietic progenitors were infected similarly on differentiation day 5 before transfer onto fresh OP9 stromal cells. HUVEC, COS-7, MCF-7, and NIH3T3 cells were infected by overnight incubation with viral supernatants at 37°C in the presence of 6 μg/mL polybrene. For long-term cultures, ES cells were selected in 10 μg/mL blasticidin (Invitrogen).

Immunostaining and fluorescence microscopy

Mouse MKs and platelets were prepared and stained as described previously[37]; other cells were grown on glass coverslips before fixation and staining. Actin stress fibers were visualized after staining with Alexa 594–conjugated phalloidin (Molecular Probes, Eugene, OR). Deconvolution microscopy followed previous description.[37] Slides were mounted with Fluoromount-G (Southern Biotech, Birmingham, AL) and examined on an Olympus (Melville, NY) IX70 inverted fluorescence microscope, using 60× (Olympus PLAN-APO 1.40 NA, 0.10 mm WD) or 100× (PLAN-APO 1.40NA, 0.10 mm WD) oil objectives or 40×/1.35 NA or 20×/0.50 plain objectives. Images were acquired with a CM350 CCD camera (Applied Precision, Issaquah, WA) using DeltaVision software (Applied Precision). Live cells were imaged using a Nikon Eclipse TE300 inverted fluorescent microscope with Nikon 10×/0.30 or 20×/0.45 plain objectives. Images acquired by a Spot camera (Diagnostic Instruments, Sterling Heights, MI) with software version 4.0.9. All images were taken at ambient temperature and processed with Photoshop 7.0 software (Adobe Systems, San Jose, CA).

Rho activity

Rho activity was assayed using a kit based on rhotekin precipitation (Cytoskeleton, Denver, CO) according to the manufacturer's instruction. Briefly, 1.5×10^6 cells were washed with phosphate-buffered saline and

From www.bloodjournal.org by guest on December 18, 2018. For personal use only.

BLOOD, 1 JULY 2007 • VOLUME 110, NUMBER 1   MYOSIN-IIA AND Rho/ROCK SIGNALS IN THROMBOPOIESIS   173

Figure 1. Myosin-IIA localization in mouse fetal liver–derived mature MKs and blood platelets. (A) Merge of actin (phalloidin, red), myosin-IIA (antibody, green), and nuclear (DAPI [4,6-diamidino-2-phenylindole], blue) staining in a representative mouse fetal liver–derived MK, with actin and myosin-IIA staining shown separately in panels Aii and Aiii, respectively. Myosin-IIA is expressed diffusely in the cytoplasm with slight increase at the cell cortex. (B-D) Myosin-IIA (green) or merge of actin (C) (red) or α-tubulin (D) (red) and myosin-IIA (green) signals in mouse fetal liver–derived proplatelets. Myosin-IIA is expressed uniformly along the proplatelet length, even though the increased cytoplasmic mass in proplatelet swellings conveys the false impression that it concentrates in these structures. Insets in panels B and C show portions of similar proplatelets at higher magnification. An organized reticular distribution is detected at the tips of individual proplatelets (D), where MK microtubules form a characteristic coil. (E) Myosin-IIA distribution in proplatelet ends resembles that seen in blood platelets. Scale bars represent 3 μm (A), 15 μm (B-C), 3 μm (B-C, insets; D), and 0.5 μm (E).
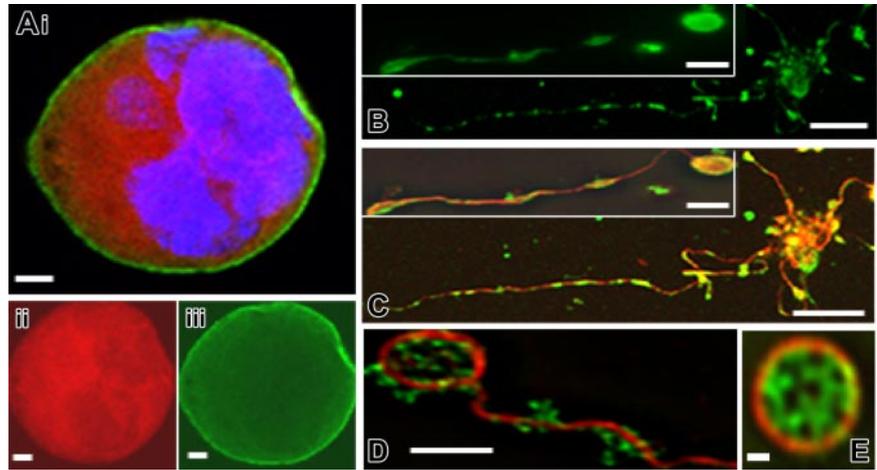
protein was extracted in 300 μL lysis buffer (25 mM Tris [tris(hydroxymethyl)aminomethane] [pH 7.5], 150 mM NaCl, 5 mM MgCl$_2$, 1% Triton X-100). Samples were centrifuged for 5 minutes at 5000g and the supernatant was incubated with rhotekin beads for 1.5 hours at 4°C. After washing the beads with buffer (25 mM Tris [pH 7.5], 40 mM NaCl, 15 mM MgCl$_2$), proteins were removed in Laemmli buffer and analyzed by immunoblotting. The ratio of rhotekin-bound RhoA and total cellular RhoA was determined using NIH Image software.

CFU-C assay of ES-derived hematopoietic progenitors

Embryoid bodies (EB) were generated from ES cells as hanging drops, as described elsewhere[38] and disaggregated on the sixth culture day. To evaluate the potential of day 6 EB-derived cells to form colonies in methylcellulose, 5×10^4 cells were plated in cytokine-enriched methylcellulose (M3434; Stem Cell Technologies). Erythroid (E), granulocyte (G), macrophage (M), mixed (GM), and multilineage (GEMM) colony-forming units (CFU) were counted 8 days later.

Results

Localization of myosin-IIA and differentiation of *MYH9* nullizygous ES cells

To elucidate myosin-IIA functions in thrombopoiesis, first we examined its subcellular localization in terminally mature MKs cultured from wild-type mice. Myosin-IIA was distributed uniformly throughout the cytoplasm, without obvious association with recognized structures. Although some cells showed apparent concentration at the cell periphery (Figure 1A), no further organization was evident. Exogenous GFP-fused myosin-IIA expressed in cultured MKs showed identical localization and seemed to function normally, as judged by association with actomyosin filaments in COS7, MCF-7, NIH3T3, and HUVEC cells (data not shown). Myosin-IIA distribution remained diffuse in MKs displaying PPF (Figure 1B-C), except at the tips of proplatelets, where it showed a reticular organization within the cytoplasm (Figure 1D). Although this pattern resembles that observed in blood platelets (Figure 1E), myosin-IIA distribution within MKs does not shed light on potential mechanisms in platelet release.

Early lethality of $Myh9^{-/-}$ embryos[31] limits in vivo investigation of the role of myosin IIA in thrombopoiesis. We therefore introduced GFP-encoding retroviruses into mouse ES cells and differentiated them toward the MK lineage in the presence of TPO and stromal cell support.[32,33] $Myh9^{+/-}$ ES cells showed robust hematopoietic and MK differentiation, indistinguishable from

$Myh9^{+/+}$ ES cells, and because $Myh9^{-/-}$ cells were derived from $Myh9^{+/-}$ clones, the latter served as the control of choice. $Myh9^{-/-}$ ES cells resisted differentiation, as reflected in increased formation of secondary embryoid bodies and reduced numbers of multipotential hematopoietic progenitors (Figure S1A). Nevertheless, MKs that did derive from $Myh9^{-/-}$ ES cells showed no overt maturational defects and generated apparently normal proplatelets (Figure 2A-C). $Myh9^{-/-}$ MKs also released platelet-like particles efficiently into the culture medium (Figure 2D-E). We confirmed that myosin-IIA is the only myosin-II isoform expressed in ES cell–derived MKs (data not shown), as demonstrated previously in bone marrow MKs.[21] Thus, substitution by close homologs cannot account for the unexpected finding that myosin-IIA is dispensable for MK differentiation and PPF.

The limited numbers of MKs derived from $Myh9^{-/-}$ cultures and their tendency to adhere to stromal cells (Figure 2C) made it difficult to acquire and interpret DNA ploidy data, but their PPF capacity implies that endomitosis is largely unaffected. Platelet-like particles released by $Myh9^{+/-}$ MKs varied substantially in size and shape (Figure S1C), and 21% to 41% of particles released by wild-type fetal liver–derived MKs with or without exogenous gene expression fall outside the flow cytometry gates defined by circulating mouse blood platelets (Figure S1D). Such heterogeneity among platelets generated in vitro highlights the limitation of culture systems to study platelet size, which is anomalous in *MYH9*-related disorders. Our experimental models nevertheless allow reliable investigation of many aspects of MK maturation and platelet release.

We consistently observed that PPF in $Myh9^{-/-}$ ES cell–derived MKs occurs more robustly than in controls (Figure 2F pie charts). This surprising result suggests that loss of myosin-IIA function enhances or accelerates platelet release and that myosin-IIA may regulate thrombopoiesis not positively but negatively. To evaluate this possibility, we treated primary cultured MKs with blebbistatin, a selective antagonist of myosin-II ATPase activity.[39] Treatment initiated at the start of fetal liver culture (ie, in blood progenitors) had no effect on the usual increase in MK size or DNA content (data not shown). However, when we exposed mature MKs to blebbistatin, PPF frequency was substantially increased (Figure 2G), again suggesting an inhibitory role for myosin-IIA.

Modeling *MYH9*-related thrombocytopenia in vivo

Patients affected by autosomal dominant *MYH9*-related disorders retain one normal allele; platelet defects may hence reflect gene
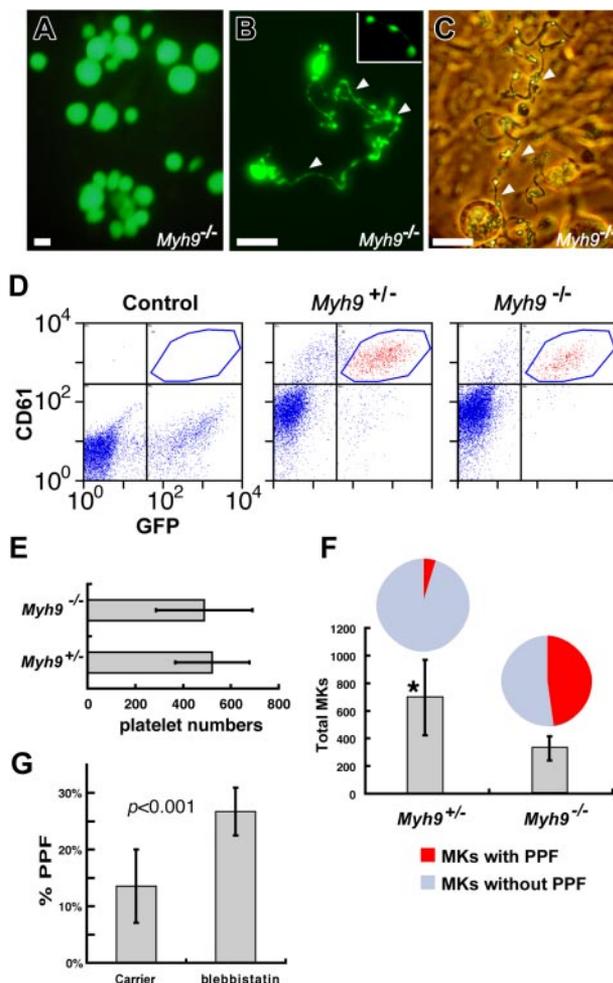
Figure 2. Myosin-IIA is not required for MK maturation in vitro. (A-C) MKs differentiated in vitro from $Myh9^{-/-}$ ES cells. (A) A representative MK colony derived from $Myh9^{-/-}$ ES cells in a day 8 differentiation culture. (B) A representative GFP-positive $Myh9^{-/-}$ MK reveals abundant proplatelets (arrowheads); the inset at top right shows a released proplatelet filament. (C) Phase-contrast image of a representative proplatelet (arrowheads)–elaborating MK from similar cultures. Bars represent 15 μm. (D) Flow cytometry analysis of platelets released by MKs differentiated from ES cells. GFP (X-axis) and CD61 (Y-axis) double-positive particles are shown in the red scattergram bounded by the blue polygon. (E) Comparison of platelet numbers released from $Myh9^{+/-}$ and $Myh9^{-/-}$ ES cell–derived MKs. Number of particles with platelet properties detected by flow cytometry within 100-μL culture supernatants are expressed per 100 PPF⁺ MKs scored visually within the same cultures. (F) Number of MKs derived from GFP-expressing $Myh9^{+/-}$ and $Myh9^{-/-}$ ES cells on differentiation day 9. Cell numbers represent MKs derived from 2×10^5 progenitors collected from day 5 differentiation culture, except that $Myh9^{+/-}$ MKs (*) are plotted at one-tenth of the original count. The pie charts above the graph represent the fraction of MKs forming proplatelets. PPF in all cultures and MKs in $Myh9^{-/-}$ samples were counted over full wells in 6-well culture dishes; $Myh9^{+/-}$ MKs were counted in 6 separate microscope fields and extrapolated to the total surface area. (G) PPF efficiency of cultured primary wild-type MKs after blockade of myosin-IIA ATPase activity. Blebbistatin (100 μM, prepared from a 20 mg/mL stock in dimethyl sulfoxide [DMSO]) or DMSO was added to fetal liver cell cultures after enrichment for MKs over a BSA step-gradient on culture day 3. PPF was assessed on day 4 as described for panel F.

haploinsufficiency or dominant-negative effects of the mutant allele. Our results with differentiated $Myh9^{+/-}$ ES cells argue against strict quantitative requirements for myosin-IIA; however, the unusually high abundance and size of this protein make it difficult to model potential dominant-negative effects of point mutations or small deletions. In contrast, GFP-labeled rod domain of myosin-IIA, an alternative dominant-negative form previously characterized in *Dictyostelium*[40] (GRD, incorporating myosin-IIA amino acids 1338–1960), was expressed more reliably than full-

length mutants in MKs, as judged by flow cytometry (data not shown), and immunoblot analysis of cultured MKs indicated 7-fold average overexpression compared with endogenous myosin-IIA (Figure S2A). We transduced wild-type mouse bone marrow cells with GRD-encoding retrovirus and infused these cells into irradiated recipient mice. Three weeks later, mice receiving GRD-transduced marrow cells showed leukocyte engraftment levels similar to those transplanted with GFP-transduced cells, but approximately one-third as many GFP-positive platelets (Figure 3A). This result confirms that interference with myosin-IIA function disrupts platelet production. Wild-type fetal liver–derived MKs expressing different myosin constructs or treated with blebbistatin showed the typical DNA ploidy profile (data not shown), which suggests that myosin-IIA functions are dispensable for endomitosis.

Gain of myosin-IIA function supports an unexpected negative role in thrombopoiesis

The broad differentiation arrest of $Myh9^{-/-}$ ES cells (Figures S1A and S2F) precluded stricter quantitative comparison of thrombopoietic efficiency. To overcome this limitation, we cultured primary mouse MKs to determine how gain of function or aberrant activity of mutant myosin-IIA might affect PPF. The numbers and morphology of proplatelets extended by cultured MKs serve as a valid physiologic marker of platelet release[19,41]; 15% to 20% of large cells usually display PPF on the fourth or fifth day after murine fetal liver progenitors are cultured in continuous presence of thrombopoietin.[30] Expression of full-length myosin-IIA in wild-type MKs delayed the period of peak PPF and reduced modestly the proportion of cells that extend proplatelets (Figure 3B). Moreover, proplatelets produced upon exogenous myosin-IIA expression displayed a distinctive, atypical morphology; nearly 70% of proplatelet-forming MKs elaborated short grape-like clusters in lieu of the extensive network of elongated filaments that appeared in most GFP-expressing control MKs (Figure S2B). These findings support the notion that myosin-IIA may act not to enable PPF, as we and others had assumed,[12] but rather to restrain it. Low viral titers and correspondingly low transduction efficiency precluded quantitative assessment of exogenous myosin-IIA levels in MKs. In $Myh9^{-/-}$ ES cells, however, the same constructs drove expression at levels comparable with those found in uninfected $Myh9^{+/-}$ ES cells (Figure S2A).

Expression of the disease-associated *MYH9* mutant R1933X in cultured MKs also attenuated PPF and delivered morphologic anomalies similar to those observed upon expression of wild-type myosin-IIA (Figure S1C), although both effects were muted in comparison with the wild-type form. Putative dominant-negative myosin-IIA forms, including R1933X, can disrupt actin stress fibers.[23] Because stress fiber detection varied considerably in our hands, even in unmanipulated wild-type MKs, we tested myosin-IIA constructs in HUVEC, where the R1933X variant did not disrupt actin stress fibers (Figure S3). Exogenous full-length myosin-IIA forms may thus function unpredictably, and we opted to study its role indirectly through its regulatory cofactors.

Regulation of myosin-IIA function in MKs

Phosphorylated myosin regulatory light chain (MLC) enhances actin-dependent myosin motor activity[24] and is thus a positive regulator whose effects should mimic gain of myosin-IIA function. We first used retroviral infection to express GFP-tagged wild type MLC in cultured murine blood progenitors and the GFP signal to

Figure 3. Interference with myosin-IIA function during MK maturation. (A) Bone marrow transplant evaluation of the role of myosin-IIA in platelet production by functional dominant interference. Control (GFP) and GFP-fused rod domain (GRD) groups represent results from 4 or 5 independently transplanted animals, and the differences in thrombopoietic efficiency are significant ($P > .02$) by the 2-tail Student t test. (B) PPF efficiency of cultured primary wild-type MKs expressing myosin-IIA constructs. Values are expressed as the fraction of all MKs (scored by cell size and morphology under phase-contrast microscopy) that extend proplatelets. Cultures were evaluated at 84 hours (black) and 96 hours (gray) after initiation of culture, and following enrichment for MKs over a BSA step-gradient.
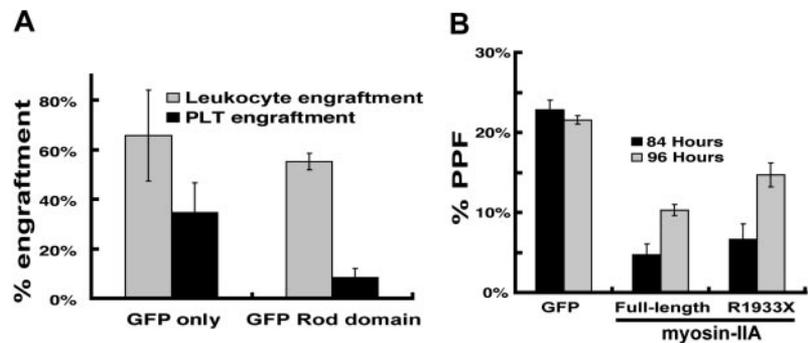
monitor infected MKs. Exogenous wild-type MLC delayed the onset of PPF by approximately 12 hours and proplatelet morphology resembled that seen with exogenous myosin-IIA expression (Figure 4A-B). Both features were more exaggerated than those obtained with myosin-IIA (Figure S1C), probably because the smaller gene construct size generated substantial MLC levels (data not shown). To test myosin gain-of-function more rigorously, we introduced a dominant-active MLC form that mimics constitutive phosphorylation ($D_{18}D_{19}$-MLC)[42,43] in hematopoietic progenitors. GFP-fused and endogenous proteins could be resolved by gel electrophoresis, and we used MLC immunoblotting to estimate that exogenous proteins were represented at an average of 1.7-fold higher level than native MLC in transduced MKs (Figure S4A). With both chicken and human $D_{18}D_{19}$-MLC constructs, genesis and maturation of MKs were unaffected but PPF was completely blocked (Figure 4A-B).

GFP-fused MLC tended to accumulate in a few spots within infected MKs (Figure 4B and data not shown). Because $D_{18}D_{19}$-MLC associated with presumptive actomyosin bundles in adherent fibroblasts from the same primary cultures (Figure 4C) and blebbistatin treatment caused the GFP signal to spread throughout the cytoplasm (data not shown), these spots likely signify regional myosin activation. Nevertheless, to exclude nonspecific toxic effects and, more important, to determine whether $D_{18}D_{19}$-MLC was acting through endogenous myosin-IIA, we expressed the constitutively active MLC (human $D_{18}D_{19}$-MLC) in $Myh9^{-/-}$ and control $Myh9^{+/-}$ ES cells. GFP signals again concentrated regionally within ES cell–derived MKs. Whereas $D_{18}D_{19}$-MLC arrested PPF in $Myh9^{+/-}$ cells, similar to effects in primary wild-type MKs, it failed to block PPF in $Myh9^{-/-}$ MKs (Figure 4D), thus establishing a clear link between $D_{18}D_{19}$-MLC actions and Myh9. In a converse test, we inhibited myosin activity by introducing a characterized, phosphorylation-resistant $A_{18}A_{19}$-MLC dominant-negative mutant[42] in primary MKs. Similar to the effect of blebbistatin, the resulting myosin-IIA inactivation enhanced PPF significantly (Figure 4A), and the majority of MKs elaborated a proplatelet network considerably more extensive than seen in typical MKs (Figure 4E). These results establish a crucial, myosin-IIA–dependent role for MLC in regulating PPF and suggest that a phospho-MLC–regulated pathway controls platelet release.

The Rho-associated kinase ROCK acts through MLC to regulate PPF negatively

Both myosin light chain kinase (MLCK) and ROCK are known to phosphorylate MLC in platelets.[44,45] To determine whether they contribute to control of PPF, we first tested the effects of the ROCK inhibitor Y27632 and the MLCK antagonist ML-7. Whereas ML-7 did not affect PPF, Y27632 enhanced PPF considerably (Figure
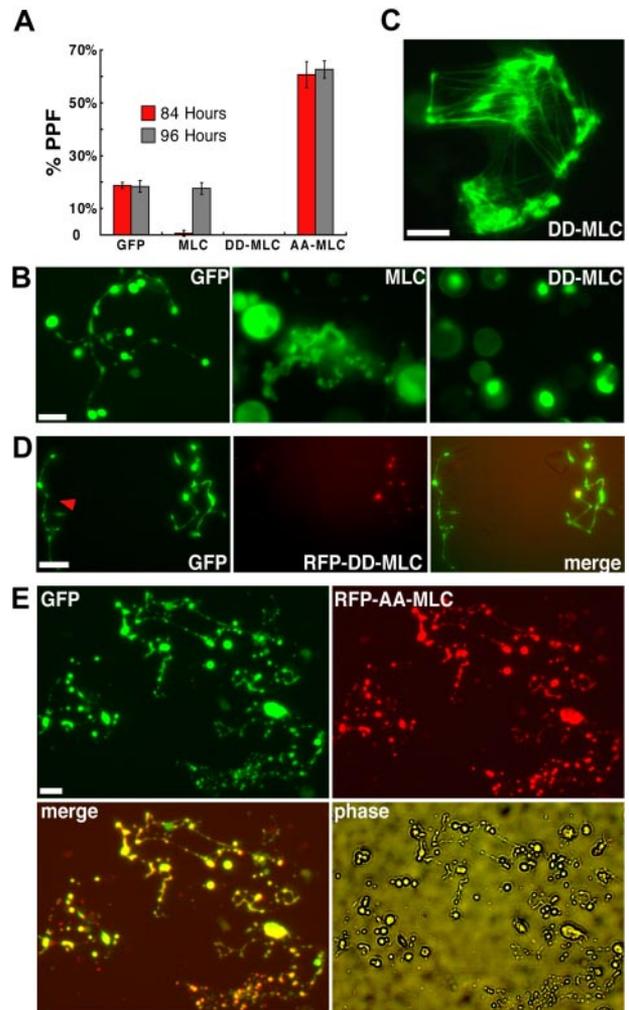

Figure 4. Myosin light chain regulates PPF negatively in a myosin-IIA–dependent manner. (A) Constitutively activated ($D_{18}D_{19}$), dominant-negative ($A_{18}A_{19}$), or wild-type GFP-tagged MLC constructs were introduced into fetal liver–derived blood progenitors by retroviral transduction. Wild-type MLC significantly delayed the onset and peak of PPF, whereas $D_{18}D_{19}$-MLC blocked PPF and $A_{18}A_{19}$-MLC enhanced PPF less than 2-fold. (B) PPF morphology after exogenous MLC expression. Abnormal grape-like clusters of proplatelets appeared with expression of wild-type MLC, compared with fully extended PPF in control GFP-expressing MKs; $D_{18}D_{19}$-MLC showed restricted localization within MKs (bright green spots) and blocked PPF. (C) GFP-$D_{18}D_{19}$-MLC incorporates into actomyosin structures formed within fibroblasts in the same primary cultures. (D) $D_{18}D_{19}$-MLC also blocked PPF in MKs derived from normal ES cells (data not shown) but not in those from $Myh9^{-/-}$ ES cells. RFP-fused $D_{18}D_{19}$-MLC was introduced by retroviral transduction into blood progenitors derived from GFP+ $Myh9^{-/-}$ ES cells on differentiation day 5 and again localized in a few spots within cells. A neighboring MK not expressing RFP-$D_{18}D_{19}$-MLC is also shown (red arrowhead). Both cells show fully extended proplatelets that appear normal. (E) $A_{18}A_{19}$-MLC enhanced PPF in wild-type MKs. MKs derived from blood progenitors doubly transduced with GFP and RFP-$A_{18}A_{19}$-MLC generated considerably more proplatelets than MKs expressing only GFP. All scale bars represent 15 μm.
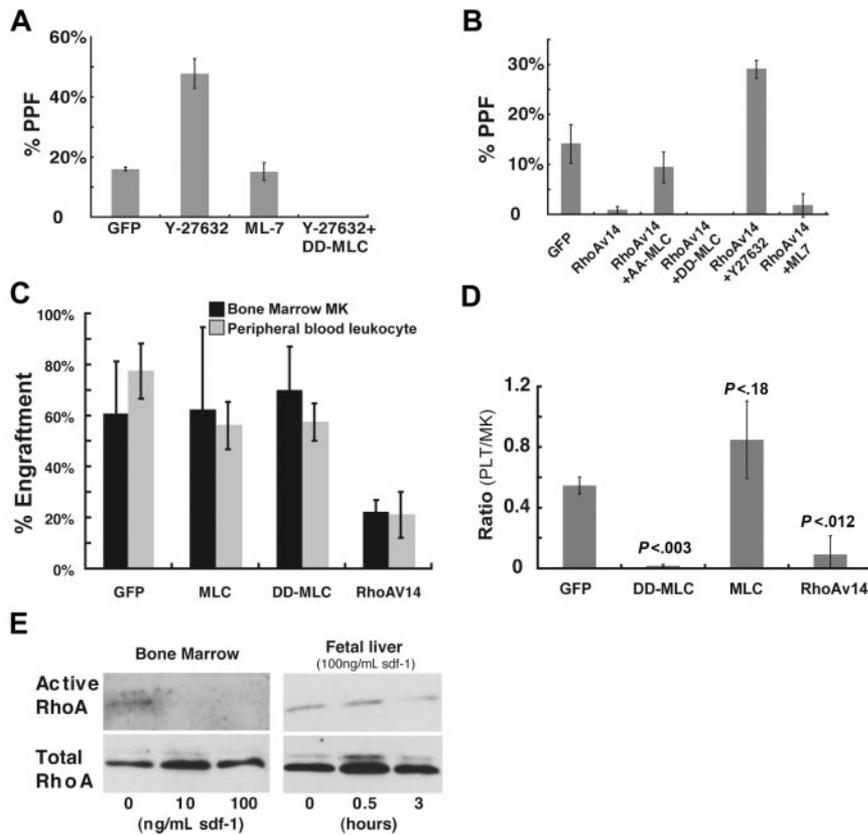
Figure 5. The small-GTPase Rho and its effector kinase ROCK control platelet production in vitro and in vivo through regulation of myosin-IIA functions. (A) MLC phosphorylation appears to be regulated by ROCK. Kinase inhibitors were added to primary MKs enriched over a BSA step-gradient on day 3 of fetal liver cell culture. PPF, assessed 24 hours later by the method described in Figure 2, was enhanced by the ROCK inhibitor Y-27632 but not the MLCK inhibitor ML-7. The effect of Y-27632 was completely reversed upon expression of $D_{18}D_{19}$-MLC. (B) Expression of activated Rho (RhoAV14) in MKs led to greatly reduced PPF, which was reversed by Y-27632 or expression of dominant-negative $A_{18}A_{19}$-MLC, but not by ML-7. (C) Mouse transplantation with blood progenitors transduced by retroviral constructs expressing wild-type MLC, $D_{18}D_{19}$-MLC, or RhoAV14. Comparison of peripheral blood leukocyte engraftment and bone marrow MK engraftment in animal groups transplanted with cells transduced by the indicated constructs. (D) Assessment of platelet production efficiency. Peripheral blood platelet recovery was measured 5 weeks after transplantation, followed by euthanasia to determine bone marrow MK and myeloid engraftment using flow cytometry. Only animals showing less than 15% MK engraftment were included in the analysis. Thrombopoietic efficiency is expressed as the ratio of (GFP^+ platelets/total platelets) to (GFP^+ MKs/total MKs). Statistical significance of the differences between groups was calculated by the 2-tailed Student t test. (E) Sdf-1 attenuates endogenous RhoA activity in mature MKs. Bone marrow–derived MKs, isolated over a BSA step-gradient 72 hours after culture initiation, were treated with 10 or 100 ng/mL recombinant Sdf-1. Activated and total Rho levels were evaluated after 3 hours. The right panel shows a time-course study of fetal liver–derived primary MKs treated with 100 ng/mL Sdf-1, with determination of Rho activity 30 minutes and 3 hours later.

5A), comparable with the increase observed upon loss of myosin-IIA activity induced by blebbistatin or $A_{18}A_{19}$-MLC. This enhancement was reversed fully in MKs expressing $D_{18}D_{19}$-MLC, which indicates that ROCK influences PPF through regulation of MLC (Figure 5A).

In many cell types, ROCK activation is regulated by the well-characterized small-GTPase Rho, which other groups have previously implicated among the signals that lead up to platelet release.[46,47] We also reported that a transcriptional program associated with Rho activity peaks in expression in MKs of mid-maturity and declines in conjunction with PPF.[48] In agreement with such results, expression of a dominant-active form of Rho (RhoAV14) reduced PPF significantly (Figure 5B) and the ROCK inhibitor Y27632 reversed this effect, increasing PPF levels even higher than those in wild-type controls. By contrast, ML-7 did not affect PPF in the context of RhoAV14, suggesting that Rho may function specifically through ROCK to control platelet release. Neither constitutively active nor dominant-negative forms of mDia1, another well-known downstream Rho effector,[29,49] influenced MK maturation or PPF (data not shown). To determine whether myosin-IIA is the principal target of Rho-ROCK signaling in regulation of PPF, we infected primary MK cultures with separate retroviruses to coexpress $A_{18}A_{19}$-MLC and RhoAV14 fused to red and green fluorescent proteins, respectively. Double-fluorescent cells displayed an average 8-fold increase in PPF compared with MKs expressing RhoAV14-GFP alone (Figures S3 and 5B). Activated MLC thus overrides the inhibition conferred on PPF by RhoAV14 and indicates that MLC is a downstream effector of Rho signaling in mature MKs. These results tightly implicate Rho and its effector kinase ROCK in PPF, first through MLC phosphorylation and secondarily through myosin-IIA functions. The data support a negative role for this pathway in thrombopoiesis.

In vivo confirmation of a mechanism for negative regulation of thrombopoiesis

To assess the in vivo significance of a putative Rho–ROCK–MLC–myosin-IIA pathway, we performed hematopoietic transplantation assays, using GFP-fused wild-type (wt)-MLC or $D_{18}D_{19}$-MLC to mimic gain of myosin-IIA function and RhoAV14 to perturb the signaling pathway at a proximal point. We transduced fetal liver cells with GFP-labeled retrovirus, infused these cells into irradiated mice, and observed equal engraftment of GFP^+ cells in circulating leukocyte and bone marrow MK populations in all experimental groups; thus, early MK differentiation is unimpaired in the presence of mutant MLC or RhoA (Figure 5C). To assess thrombopoiesis, we measured the ratio of fluorescent platelets to GFP-expressing MKs. Mice rescued with cells that express either GFP alone or GFP-wt MLC yielded at least 1:2 ratios between fluorescent platelets and engrafted MKs. In contrast, cells transduced with either dominant-active $D_{18}D_{19}$-MLC or dominant-active RhoAV14 showed few GFP-positive platelets relative to robust MK engraftment in bone marrow (Figure 5D). Both $D_{18}D_{19}$-MLC (Figure 4) and RhoAV14 (Figure 5B) blocked PPF in cultured MKs, whereas exogenous MLC delayed but did not obviate the process (Figure 4A). Marrow transplantation results are thus fully concordant with those from MK culture.

A candidate extracellular regulator of Rho function in MKs

Our data place myosin-IIA in a pathway that responds to external cues and conveys signals through Rho and ROCK to restrain platelet release. Of the many cytokines present in marrow stroma, Sdf-1/CXCL12 is both a MK chemoattractant[14-16] and a regulator of Rho activity during neurite outgrowth,[29] a process that superficially resembles PPF. To assess the plausibility of a model wherein

Sdf-1 regulates the Rho-ROCK-myosin pathway in MKs, we treated cultured cells from 2 different sources with recombinant Sdf-1. Mouse bone marrow– and fetal liver–derived MKs responded to Sdf-1 with measurable reduction of cellular Rho activity (Figure 5E). This response varied with both Sdf-1 concentration and the duration of exposure.

Discussion

The functional outcome of MK maturation is the assembly and release of thousands of blood platelets, a final step that is preceded by obligate changes in MK shape and cytoskeletal organization.[19,20] We outline a cell-intrinsic signaling pathway that seems to restrain PPF and converges on myosin-IIA *(Myh9)*, an abundant nonmuscle myosin in MKs and platelets. Because myosin-II isoforms control shape in other cell types and couple morphogenesis with cytoskeletal rearrangements,[1-3] they are good candidates to mediate cytoskeletal or motor functions related to platelet release. Although it is therefore commonly assumed that myosin-IIA enables thrombopoiesis,[12] our data suggest that, on the contrary, myosin-IIA may act to limit platelet release. Thus, PPF is enhanced in MKs derived from *Myh9*$^{-/-}$ ES cells, in primary MKs treated with the myosin-ATPase inhibitor blebbistatin, and upon dominant interference with either myosin-IIA or its regulator MLC. Most important, the phospho-MLC–mimetic $D_{18}D_{19}$-MLC, which activates myosin,[43] attenuates PPF in cultured MKs and those differentiated from *Myh9*$^{+/-}$ ES cells but not in MKs derived from *Myh9*$^{-/-}$ ES cells. These results collectively implicate myosin-IIA and its upstream signaling pathway in negative regulation of platelet release.

MKs are very likely to require mechanisms to avoid platelet assembly and release until the appropriate time. Following endomitosis, the MK cytoplasm gradually accumulates the many molecules and organelles that need to be packaged within each platelet; as these components are produced asynchronously, some will remain limiting until the cell is fully mature. Precocious platelet assembly would result either in faulty structures with a paucity of the limiting ingredients or, when critical material is lacking, in MKs failing to realize their full synthetic potential. If most MKs produce platelets prematurely, the predicted outcome is thrombocytopenia, and our results imply that this may be a basis for the May-Hegglin and related *MYH9*-associated disorders. We suggest that myosin-IIA is a critical element in a pathway that restrains thrombopoiesis until MKs accumulate sufficient quantities of the materials required to assemble platelets optimally. Sabri et al[41] recently argued for a conceptually similar basis for thrombocytopenia associated with the Wiskott-Aldrich syndrome, where observations in mice suggested platelet release occurs in the marrow interstitium instead of the sinusoidal vasculature.

Because platelet assembly and release are coupled processes,[20] our model accounts for the heterogeneous platelet populations observed in *MYH9*-related disorders: prematurely released platelets might escape fine control over their final size, and limitation of elements required to confer elliptical shape, such as the MK-specific tubulin isoform β1,[50] might induce spherocytosis in a platelet subpopulation. Notably, MKs would still produce many normal or nearly normal platelets and hemostasis may not be significantly compromised, exactly as reported in humans with *MYH9* gene mutations. *MYH9* mutations that result in either gain or loss of function could, in principle, affect thrombopoiesis adversely. Loss of myosin-IIA function could trigger PPF prematurely, whereas gain-of-function mutations may limit platelet

production. *MYH9* mutations in humans are distributed across the coding region and there is no correlation between genotypes and the spectrum of clinical manifestations.[21,51] Thrombocytopenia is the one common feature among *MYH9*-associated disorders and it will be interesting to study MK anomalies in relation to our model and to specific mutations, although patient-derived materials could be a limiting factor.

Compared with the largely invariant size distribution of normal blood platelets, those released from cultured MKs are very heterogeneous, even when gene expression is not manipulated. In culture, constitutive inhibition of PPF, as we propose occurs in vivo, is probably lacking or inefficient; accordingly, platelet release may be generally premature and favor heterogeneity in size and shape. Platelet size is also highly variable for several weeks after bone marrow transplantation, even in mice receiving untransduced cells. Although our studies provided reliable handles on PPF and circulating platelet numbers, these features curtailed our ability to assess platelet size, a parameter that is defective in the May-Hegglin anomaly.

The *MYH9*-associated disorders, which are inherited as autosomal dominant traits, must reflect either gene haploinsufficiency or dominant-negative effects of the mutant allele. In vitro differentiation of *Myh9*$^{+/-}$ mouse ES cells suggest that gene dosage is unlikely to be a limiting factor in humans but this remains formally possible for some truncation mutants. The extreme abundance of endogenous myosin-IIA and the technical challenges associated with exogenous expression of common mutant forms, which are large, make it difficult to establish the nature of likely dominant-negative effects. We therefore used $D_{18}D_{19}$-MLC as a means to activate myosin-IIA and then extended the studies to reveal apparent regulation of myosin-IIA by MLC, Rho, and ROCK. Transplantation experiments confirmed the importance of this signaling pathway, because platelet numbers fell upon functional interference through the myosin-IIA C-terminal rod domain (Figure 3A) and with constructs that mimic phospho-MLC or constitutively active Rho (Figure 5D).

Our studies complement and extend elements of a report that appeared while this manuscript was in preparation. Using MKs differentiated in vitro from cord blood and adult human CD34$^+$ cells, Chang et al[47] show that Rho and ROCK are negative regulators of PPF. Their study began with assessment of Rho activity in maturing MKs and led them to speculate that the Rho-ROCK pathway may impinge on myosin-IIA regulation of platelet release. By contrast, our study originated in a quest to decipher the cellular basis of *MYH9*-related disorders. We used genetic tools (*Myh9*-null ES cells) and exogenous gene expression in cultured mouse MKs to infer that myosin-IIA may inhibit rather than enable platelet release. Working from this observation, we investigated the mechanisms that may regulate myosin-IIA motor activity, including MLC and potential MLC kinases. Our conclusions, based on precise combinations of genetic tools, exogenous constructs, and small-molecule antagonists, argue for an inhibitory role for the Rho–ROCK–MLC–myosin-IIA pathway in thrombopoiesis. The 2 reports thus reinforce each other's conclusions and together set the stage for further mechanistic investigation of thrombopoietic mechanisms in general and defects underling *MYH9*-related disorders in particular.

Our model emphasizes a role for continuous inhibition of PPF during MK maturation. Factors like collagen I found in the marrow environment may activate Rho GTPase continuously in MKs and thus inhibit PPF. In the final maturation stage, MKs migrate to a different niche, near vascular endothelium, where Sdf-1 and other

factors may act to lift the restraints imposed by the Rho-ROCK-myosin pathway and hence enable PPF (Figure S5). Signals that trigger PPF in preterminal MKs are poorly understood, and although there may be several, the link to Rho signaling highlights the potential role of Sdf-1/CXCL12, a known MK chemoattractant[14-16] and an extracellular ligand known to signal to Rho.[29] Advanced MKs respond to Sdf-1 with reduced cellular Rho activity (Figure 5E), a change that would reverse the proposed inhibition of PPF by ROCK and phospho-MLC. Sdf-1 is enriched in marrow sinusoids, where terminally mature MKs are known to home.[13] Acting in concert with other local factors, Sdf-1 may attenuate MK Rho activity and hence trigger PPF. Investigation of these possibilities will improve understanding of homeostatic mechanisms that maintain constant platelet numbers in the circulation while meeting the body's continuous demand to replenish cleared platelets.

Acknowledgments

Authorship

Contribution: Z.C., O.N., A.B., A.M., and R.A.S. designed and performed the research; M.A.C. and R.S.A. provided essential reagents; Z.C., O.N., A.B., A.M., D.I., G.Q.D., and R.A.S. interpreted and analyzed the data; and Z.C. and R.A.S. wrote the paper. A.B. and O.N. contributed equally to this study.

Conflict-of-interest disclosure: The authors declare no competing financial interests.

Correspondence: Ramesh A. Shivdasani, Dana-Farber Cancer Institute, One Jimmy Fund Way, Boston, MA 02115; e-mail: ramesh_shivdasani@dfci.harvard.edu.

References

1. van Leeuwen FN, van Delft S, Kain HE, van der Kammen RA, Collard JG. Rac regulates phosphorylation of the myosin-II heavy chain, actinomyosin disassembly and cell spreading. Nat Cell Biol. 1999;1:242-248.

2. Paterson HF, Self AJ, Garrett MD, Just I, Aktories K, Hall A. Microinjection of recombinant p21rho induces rapid changes in cell morphology. J Cell Biol. 1990;111:1001-1007.

3. Franke JD, Montague RA, Kiehart DP. Nonmuscle myosin II generates forces that transmit tension and drive contraction in multiple tissues during dorsal closure. Curr Biol. 2005;15:2208-2221.

4. Seri M, Cusano R, Gangarossa S, et al. Mutations in MYH9 result in the May-Hegglin anomaly, and Fechtner and Sebastian syndromes. The May-Hegglin/Fechtner Syndrome Consortium. Nat Genet. 2000;26:103-105.

5. Kunishima S, Kojima T, Matsushita T, et al. Mutations in the NMMHC-A gene cause autosomal dominant macrothrombocytopenia with leukocyte inclusions (May-Hegglin anomaly/Sebastian syndrome). Blood. 2001;97:1147-1149.

6. Kelley MJ, Jawien W, Ortel TL, Korczak JF. Mutation of MYH9, encoding non-muscle myosin heavy chain A, in May-Hegglin anomaly. Nat Genet. 2000;26:106-108.

7. May R. Leukocyteneinschlusse. Dtsch Arch Klin Med. 1909;96:1-6.

8. Hegglin R. Simultaneous constitutional changes in neutrophils and platelets. Helv Med Acta. 1945;12:439-440.

9. Noris P, Spedini P, Belletti S, Magrini U, Balduini CL. Thrombocytopenia, giant platelets, and leukocyte inclusion bodies (May-Hegglin anomaly): clinical and laboratory findings. Am J Med. 1998;104:355-360.

10. Hamilton RW, Shaikh BS, Ottie JN, Storch AE, Saleem A, White JG. Platelet function, ultrastructure, and survival in the May-Hegglin anomaly. Am J Clin Pathol. 1980;74:663-668.

11. Godwin HA, Ginsburg AD. May-Hegglin anomaly: a defect in megakaryocyte fragmentation? Br J Haematol. 1974;26:117-128.

12. Balduini CL, Savoia A. Inherited thrombocytopenias: molecular mechanisms. Semin Thromb Hemost. 2004;30:513-523.

13. Lichtman MA, Chamberlain JK, Simon W, Santillo PA. Parasinusoidal location of megakaryocytes in marrow: a determinant of platelet release. Am J Hematol. 1978;4:303-312.

14. Lane WJ, Dias S, Hattori K, et al. Stromal-derived factor 1-induced megakaryocyte migration and platelet production is dependent on matrix metalloproteinases. Blood. 2000;96:4152-4159.

15. Avecilla ST, Hattori K, Heissig B, et al. Chemokine-mediated interaction of hematopoietic progenitors with the bone marrow vascular niche is required for thrombopoiesis. Nat Med. 2004;10:64-71.

16. Berthebaud M, Riviere C, Jarrier P, et al. RGS16 is a negative regulator of SDF-1-CXCR4 signaling in megakaryocytes. Blood. 2005;106:2962-2968.

17. Radley JM, Scurfield G. The mechanism of platelet release. Blood. 1980;56:996-999.

18. Choi ES, Nichol JL, Hokom MM, Hornkohl AC, Hunt P. Platelets generated in vitro from proplatelet-displaying human megakaryocytes are functional. Blood. 1995;85:402-413.

19. Italiano JE Jr, Lecine P, Shivdasani RA, Hartwig JH. Blood platelets are assembled principally at the ends of proplatelet processes produced by differentiated megakaryocytes. J Cell Biol. 1999;147:1299-1312.

20. Italiano JE Jr, Shivdasani RA. Megakaryocytes and beyond: the birth of platelets. J Thromb Haemost. 2003;1:1174-1182.

21. Marigo V, Nigro A, Pecci A, et al. Correlation between the clinical phenotype of MYH9-related disease and tissue distribution of class II nonmuscle myosin heavy chains. Genomics. 2004;83:1125-1133.

22. Hu A, Wang F, Sellers JR. Mutations in human nonmuscle myosin IIA found in patients with May-Hegglin anomaly and Fechtner syndrome result in impaired enzymatic function. J Biol Chem. 2002;277:46512-46517.

23. Franke JD, Dong F, Rickoll WL, Kelley MJ, Kiehart DP. Rod mutations associated with MYH9-related disorders disrupt nonmuscle myosin-IIA assembly. Blood. 2005;105:161-169.

24. Bresnick AR. Molecular mechanisms of nonmuscle myosin-II regulation. Curr Opin Cell Biol. 1999;11:26-33.

25. Fujita A, Saito Y, Ishizaki T, et al. Integrin-dependent translocation of p160ROCK to cytoskeletal complex in thrombin-stimulated human platelets. Biochem J. 1997;328:769-775.

26. Schoenwaelder SM, Hughan SC, Boniface K, et al. RhoA sustains integrin $\alpha_{IIb}\beta_3$ adhesion contacts under high shear. J Biol Chem. 2002;277:14738-14746.

27. Wilde JI, Retzer M, Siess W, Watson SP. ADP-induced platelet shape change: an investigation of the signalling pathways involved and their dependence on the method of platelet preparation. Platelets. 2000;11:286-295.

28. Chalasani SH, Sabelko KA, Sunshine MJ, Littman DR, Raper JA. A chemokine, SDF-1, reduces the effectiveness of multiple axonal repellents and is required for normal axon pathfinding. J Neurosci. 2003;23:1360-1371.

29. Arakawa Y, Bito H, Furuyashiki T, et al. Control of axon elongation via an SDF-1α/Rho/mDia pathway in cultured cerebellar granule neurons. J Cell Biol. 2003;161:381-391.

30. Tiwari S, Italiano JE Jr, Barral DC, et al. A role for Rab27b in NF-E2-dependent pathways of platelet formation. Blood. 2003;102:3970-3979.

31. Conti MA, Even-Ram S, Liu C, Yamada KM, Adelstein RS. Defects in cell adhesion and the visceral endoderm following ablation of nonmuscle myosin heavy chain II-A in mice. J Biol Chem. 2004;279:41263-41266.

32. Eto K, Murphy R, Kerrigan SW, et al. Megakaryocytes derived from embryonic stem cells implicate CalDAG-GEFI in integrin signaling. Proc Natl Acad Sci U S A. 2002;99:12819-12824.

33. Fujimoto TT, Kohata S, Suzuki H, Miyazaki H, Fujimura K. Production of functional platelets by differentiated embryonic stem (ES) cells in vitro. Blood. 2003;102:4044-4051.

34. Villeval JL, Cohen-Solal K, Tulliez M, et al. High thrombopoietin production by hematopoietic cells induces a fatal myeloproliferative syndrome in mice. Blood. 1997;90:4369-4383.

35. Phillips LL, Malm JR. Coagulation changes after perfusion with heparinized blood and ACD blood buffered with tris (hydroxy methyl) amino methane. Bibl Haematol. 1968;29:858-862.

36. Naviaux RK, Costanzi E, Haas M, Verma IM. The

pCL vector system: rapid production of helper-free, high-titer, recombinant retroviruses. J Virol. 1996;70:5701-5705.

37. Schulze H, Korpal M, Hurov J, et al. Characterization of the megakaryocyte demarcation membrane system and its role in thrombopoiesis. Blood. 2006;107:3868-3875.

38. Wang Y, Yates F, Naveiras O, Ernst P, Daley GQ. Embryonic stem cell-derived hematopoietic stem cells. Proc Natl Acad Sci U S A. 2005;102:19081-19086.

39. Straight AF, Cheung A, Limouze J, et al. Dissecting temporal and spatial control of cytokinesis with a myosin II inhibitor. Science. 2003;299:1743-1747.

40. Burns CG, Larochelle DA, Erickson H, Reedy M, De Lozanne A. Single-headed myosin II acts as a dominant negative mutation in *Dictyostelium*. Proc Natl Acad Sci U S A. 1995;92:8244-8248.

41. Sabri S, Foudi A, Boukour S, et al. Deficiency in the Wiskott-Aldrich protein induces premature proplatelet formation and platelet production in the bone marrow compartment. Blood. 2006;108:134-140.

42. Fumoto K, Uchimura T, Iwasaki T, Ueda K, Hosoya H. Phosphorylation of myosin II regulatory light chain is necessary for migration of HeLa cells but not for localization of myosin II at the leading edge. Biochem J. 2003;370:551-556.

43. Ward Y, Yap SF, Ravichandran V, et al. The GTP binding proteins Gem and Rad are negative regulators of the Rho-Rho kinase pathway. J Cell Biol. 2002;157:291-302.

44. Amano M, Mukai H, Ono Y, et al. Identification of a putative target for Rho as the serine-threonine kinase protein kinase N. Science. 1996;271:648-650.

45. Gallagher PJ, Herring BP, Griffin SA, Stull JT. Molecular characterization of a mammalian smooth muscle myosin light chain kinase. J Biol Chem. 1991;266:23936-23944.

46. Sabri S, Jandrot-Perrus M, Bertoglio J, et al. Differential regulation of actin stress fiber assembly and proplatelet formation by $\alpha2\beta1$ integrin and GPVI in human megakaryocytes. Blood. 2004;104:3117-3125.

47. Chang Y, Aurade F, Larbret F, et al. Proplatelet formation is regulated by the Rho/ROCK pathway. Blood. 2007;109:4229-4236.

48. Chen Z, Hu M, Shivdasani RA. Expression analysis of primary mouse megakaryocyte differentiation and its application to identify stage-specific molecular markers and a novel transcriptional target of NF-E2. Blood. 2007;109:1451-1459.

49. Watanabe N, Kato T, Fujita A, Ishizaki T, Narumiya S. Cooperation between mDia1 and ROCK in Rho-induced actin reorganization. Nat Cell Biol. 1999;1:136-143.

50. Schwer HD, Lecine P, Tiwari S, Italiano JE Jr, Hartwig JH, Shivdasani RA. A lineage-restricted and divergent β-tubulin isoform is essential for the biogenesis, structure and function of blood platelets. Curr Biol. 2001;11:579-586.

51. Dong F, Li S, Pujol-Moix N, et al. Genotype-phenotype correlation in MYH9-related thrombocytopenia. Br J Haematol. 2005;130:620-627.

The May-Hegglin anomaly gene *MYH9* is a negative regulator of platelet biogenesis modulated by the Rho-ROCK pathway

Zhao Chen, Olaia Naveiras, Alessandra Balduini, Akiko Mammoto, Mary Anne Conti, Robert S. Adelstein, Donald Ingber, George Q. Daley and Ramesh A. Shivdasani